AERODYNAMIC ANALYSIS OF THE HELICOPTER ROTOR USING THE TIME-DOMAIN PANEL METHOD

Seawook Lee*, Hyunmin Choi*, Leesang Cho*, Jinsoo Cho**
* Department of Mechanical Engineering, Hanyang Univeristy, Seoul, Korea
** School of Mechanical Engineering, Hanyang University, Seoul, Korea

Keywords: *Aerodynamic Analysis, Helicopter Rotor, Panel Method, Free Wake*

Abstract

The paper presents the unsteady aerodynamic analysis of helicopter rotor with a panel method based on potential flow theory. The panel method uses the piecewise constant source and doublet singularities as a solution. This potential based panel method is founded on the Dirichlet boundary condition and coupled with the time-stepping method. The present method is used the time-stepping loop to simulate the unsteady motion of the helicopter rotor. And the free wake model is used for the wake simulation. The present method can be solved the three-dimensional flow over the complex rotors with less computing time than commercial CFD tools. The results are well matched with the experimental results. That will do much for practical applications such as aerodynamic designs and analysis of helicopter rotor configurations.

1 Introduction

Currently, most nations use helicopters in military and industrial fields. A helicopter can be defined as any flying machine using rotating wings to provide lift, propulsion, and control forces[1,2]. A Helicopter can forward flight and hovering using the rotation of helicopter rotor.

The research on the aerodynamic characteristics of the helicopter rotor has been performed broadly. Although there were great amount of efforts that have developed the helicopter, only few countries have their own helicopters and design technology. Compared to fixed wing aircraft, the helicopter has highly complex aerodynamic characteristics. Therefore, a large amount of both experimental tests and numerical analyses must be performed with hovering and forward flight conditions.

Aerodynamic performance of the helicopter rotor is determined by the compressibility, flow separation, blade tip vortex and blade-vortex interaction.

In this research, aerodynamic analysis and wake simulation of the helicopter rotor were performed using the time-domain panel method and free wake.

2 Numerical Method

2.1 Governing Equation

The flow is assumed to be invicid, irrotational, and incompressible. Hence, a velocity potential $\Phi(x, y, z)$ can be defined, and continuity equation becomes Laplace's equation:

$$\nabla^2 \Phi = 0, \ \vec{V} = \nabla \Phi \qquad (1)$$

The general solution to Eq. (1) can be constructed, based on Green's identity, by a sum of source σ and doublet μ distributions on all of the known boundaries[3].

$$\Phi(P) = -\frac{1}{4\pi} \iint_{body} \sigma \frac{1}{r} - \mu \frac{\partial}{\partial n}\left(\frac{1}{r}\right) dSz$$
$$+ \frac{1}{4\pi} \iint_{wake} \mu \frac{\partial}{\partial n}\left(\frac{1}{r}\right) dS + \Phi_\infty(P) \qquad (2)$$

To impose the Dirichlet boundary condition on the surface, the perturbation

potential has to be specified everywhere on the body. If for an enclosed body $\partial\Phi/\partial n = 0$, then the potential inside the body will not change. Thus, Eq. (2) becomes as follow.

$$\begin{aligned}\Phi(P) = &-\frac{1}{4\pi}\iint_{body}\sigma\frac{1}{r}dS \\ &+\frac{1}{4\pi}\iint_{body}\mu\frac{\partial}{\partial n}\left(\frac{1}{r}\right)dS \\ &+\frac{1}{4\pi}\iint_{wake}\mu\frac{\partial}{\partial n}\left(\frac{1}{r}\right)dS = 0\end{aligned} \tag{3}$$

The unsteady motion are expressed using the boundary condition on the surface of object due to no time-term in the Eq. (1)

$$\frac{\partial\Phi}{\partial n} = \left(V_O + v_{rel} + \Omega\times r\right)\cdot n = 0 \tag{4}$$

Where v_{rel} is the relative velocity on the body fixed coordinate and r is indicated as a position of panel control point.

2.2 Flight Path and Rotational Information

As the shown Fig. 1, (X,Y,Z) is determined as a inertial coordinate system, and (x,y,z) is considered as a body fixed coordinate. Therefore, the path of origin R and rotational information Θ can be combined with forwarding mode and vibration mode. Then this is expressed as below.

$$\begin{aligned}R_o(t) &= -Q_\infty t + A\sin(\omega t - v) \\ \Theta(t) &= -\zeta t + A\sin(\omega t - v)\end{aligned} \tag{5}$$

Now, the velocity V_o and angular velocity Ω can be written as the Eq. (6)

$$\begin{aligned}V_o(t) &= -Q_\infty + A\omega\cos(\omega t - v) \\ \Omega(t) &= -\zeta + A\omega\cos(\omega t - v)\end{aligned} \tag{6}$$

At this point, free flow velocity, constant angular velocity, amplitude of vibration, frequency, and angle of delay are shown as Q_∞, ζ, A, ω, and v respectively.
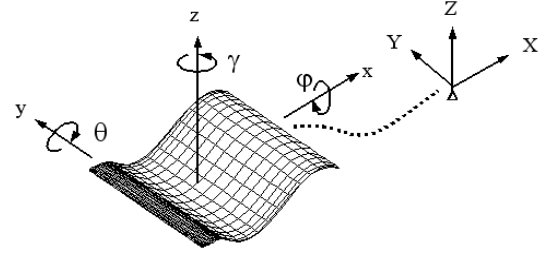

Fig. 1. Inertial and body coordinates used to describe the motion of the body

To estimate the transformation of coordinate, the equation of transformation was shown as below.

$$\begin{aligned}\begin{pmatrix}x\\y\\z\end{pmatrix} = &\begin{pmatrix}1 & 0 & 0\\0 & \cos\phi(t) & \sin\phi(t)\\0 & -\sin\phi(t) & \cos\phi(t)\end{pmatrix} \\ &\begin{pmatrix}\cos\theta(t) & 0 & -\sin\theta(t)\\0 & 1 & 0\\\sin\theta(t) & 0 & \cos\theta(t)\end{pmatrix} \\ &\begin{pmatrix}\cos\psi(t) & \sin\psi(t) & 0\\-\sin\psi(t) & \cos\psi(t) & 0\\0 & 0 & 1\end{pmatrix}\begin{pmatrix}X-X_0\\Y-Y_0\\Z-Z_0\end{pmatrix}\end{aligned} \tag{7}$$

2.3 Wake

To sophisticated unsteady motion at the trailing edge or entire flow, the wake that flows from separation point which is determined by user is created by addition of wake panels at each time interval Δt. The strengths of doublet at the wake-panel is computed with Morino Kutta condition each time and their strengths would be maintained along the time by the determination of Helmholtz[4].

$$\Phi_{wake} = \Phi_{upper} - \Phi_{lower} \tag{8}$$

The new strength of wake was determined by the average value of the previous strength of wake as given in Eq. (9). Hence, The Kutta condition can be applied more accurately and the pressure gradient can be minimized[5].

$$\Phi_{average} = \frac{\Phi_{wake}(t) + \Phi_{wake}(t-\Delta t)}{2} \tag{9}$$

2.4 Calculation Velocity and Pressure

The tangential velocity and the perturbation velocity are obtained at each panel as follow.

$$v_l = \frac{\partial \mu}{\partial l}, \ v_m = \frac{\partial \mu}{\partial m} \qquad (10)$$

The perturbation velocity of normal direction is shown as below.

$$v_n = -\sigma \qquad (11)$$

Normally, the perturbation velocity on the tangential direction is obtained using the central difference method, can be obtained by Eq. (12)

$$\begin{aligned} v_l &= \frac{\partial \mu}{\partial l} = \frac{1}{2\Delta l}(\mu_{l+1} - \mu_{l-1}) \\ v_m &= \frac{\partial \mu}{\partial m} = \frac{1}{2\Delta m}(\mu_{m+1} - \mu_{m-1}) \end{aligned} \qquad (12)$$

However, due to the arbitrary shape, it is not useful to calculate with the difference method. In this paper, the VSAERO's [6] polynomial interpolation which has been used in the commercial panel code broadly was adopted to obtain the tangential velocity and the sum of the perturbation velocity plus local kinematic velocity which is the local fluid velocity as given in Eq. (13)

$$Q_k = V_{kine} \cdot (l,m,n)_k + (v_l, v_n, v_m)_k \qquad (13)$$

Where $(l,m,n)_k$ are the local tangential and normal directions and the components of V_{kine} in these directions are obtained and V_{kine} is the magnitude of the kinematic velocity as follow.

$$V_{kine} = -(V_o + v_{rel} + \Omega \times r) \qquad (14)$$

The local perturbation velocity is $(v_l, v_n, v_m) = (\partial \Phi / \partial l, \quad \partial \Phi / \partial m, \ \partial \Phi / \partial n)$ and of course the normal velocity component on the solid body is zero. The pressure coefficient can now be carried out for each panel as follow.

$$C_P = \frac{p - p_{kine}}{\frac{1}{2}\rho v_{kine}^2} 1 - \frac{Q^2}{V_{kine}^2} - \frac{2}{V_{kine}^2}\frac{\partial \Phi}{\partial t} \qquad (15)$$

2.5 Wake Rollup

The local velocity is related with the motion of the object. The wake rollup at each time step can be performed and each vortex of the wake both trailing edge and separated will move with the local velocity $(u, v, w,)_l$ by the amount.

$$(u, v, w,)_l = (u, v, w,)_{l,body} + (u, v, w,)_{l,wake} \qquad (16)$$

$$(\Delta X, \Delta Y, \Delta Z)_l = (u, v, w,)_l \cdot \Delta t \qquad (17)$$

$$\begin{bmatrix} X \\ Y \\ Z \end{bmatrix}_l = \begin{bmatrix} X \\ Y \\ Z \end{bmatrix}_l + \begin{pmatrix} \Delta X \\ \Delta Y \\ \Delta Z \end{pmatrix}_l \qquad (18)$$

The local perturbation velocity is $(v_l, v_n, v_m) = (\partial \Phi / \partial l)$

3 Results

3.1 Hovering

Figure 2 shows F. X. Caradonna and C. Tung's rotor[7]. Diameter of the rotor is 2.286m, aspect ratio AR=6, and sectional airfoil shape is NACA 0012. Rotational speed is 1,250~2,250 RPM, collective pitch is 5~12 degree, and flight speed is 0 m/s (hovering).

Figure 3 shows the F. X. Caradonna and C. Tung's rotor paneling for the calculation the rotor performances using present method. Present method was assumed incompressible, and inviscid conditions. In rotor tip, from rotational speed and forward speed, compressible effect is considered seriously. Therefore Prandtl-Glauert's rule was used to

consider the compressible effect in present method.

Figure 4~12 shows the pressure distributions from mid-span(a) to tip(d). Fig. 4 is the results pressure distribution when the rotational speed is 1,250 RPM, and collective pitch is 5 degree. Fig. 5 is the results pressure distribution when the rotational speed is 1,250 RPM, and collective pitch is 8 degree. Fig. 6 is the results pressure distribution when the rotational speed is 1,250 RPM, and collective pitch is 12 degree. Fig. 7 is the results pressure distribution when the rotational speed is 1,750 RPM, and collective pitch is 5 degree. Fig. 8 is the results pressure distribution when the rotational speed is 1,750 RPM, and collective pitch is 8 degree. Fig. 9 is the results pressure distribution when the rotational speed is 1,750 RPM, and collective pitch is 12 degree. Fig. 10 is the results pressure distribution when the rotational speed is 2,250 RPM, and collective pitch is 5 degree. Fig. 11 is the results pressure distribution when the rotational speed is 2,250 RPM, and collective pitch is 8 degree. Fig. 12 is the results pressure distribution when the rotational speed is 2,250 RPM, and collective pitch is 12 degree.

In (a) of all figures of present method matched well compared to the results of experiment. Because the speed of (a) (r/R=0.5) is lower than the tip speed. So the results between with Prandtl-Glauert's rule and without Prandtl-Glauert's rule of present method matched well with the results of experiment. But there was some difference at tip. But, in (d) of all figures of present method have a difference respectively. Because the (d) position is the rotor blade tip region. In those regions, tip Mach number is in the consideration region of compressible effect. The results of present method is not matched exactly neverthe less using the Prandtl-Glauert's rule.

Table 1 shows the results of present method and F. X. Caradonna and C. Tung. When rotational speed and collective pitch were increased, the deviation of thrust coefficient was increased.

Figure 13~15 show the wake shapes of each case using the present method. To prevent wake pass through the solid bodies(rotor), the close approach method was used.
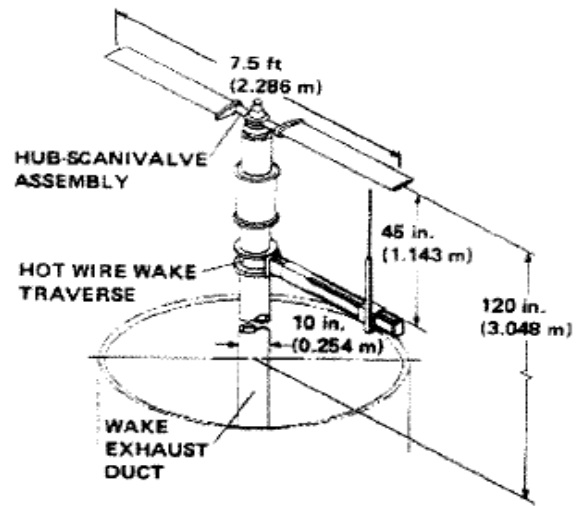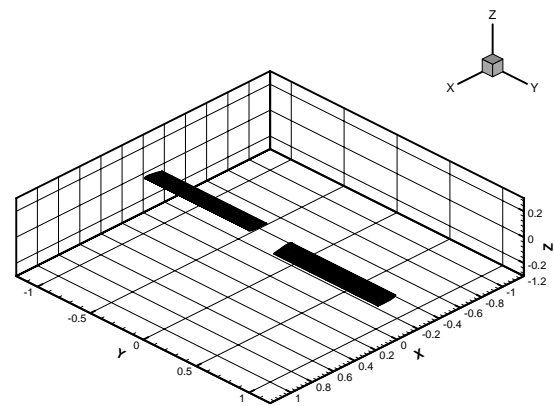

Fig. 2. F.X. Caradonna and C. Tung's Rotor

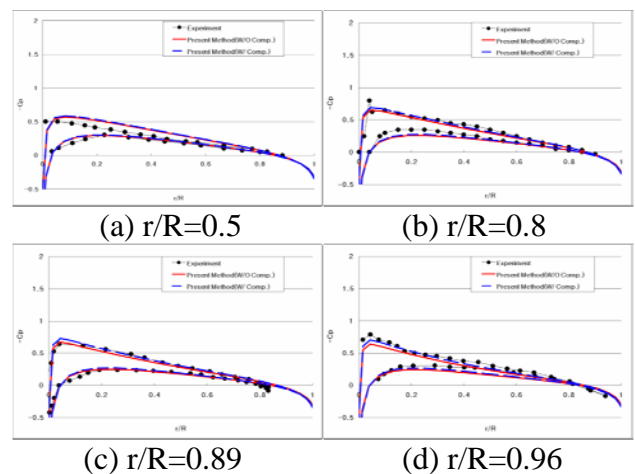Fig. 3. Paneling of the F.X. Caradonna and C. Tung's Rotor

(a) r/R=0.5   (b) r/R=0.8

(c) r/R=0.89   (d) r/R=0.96
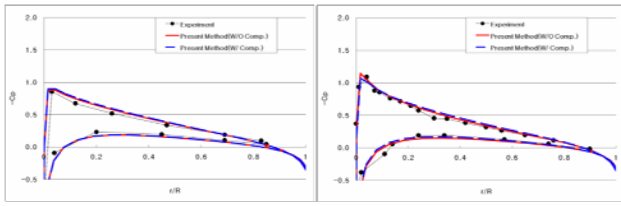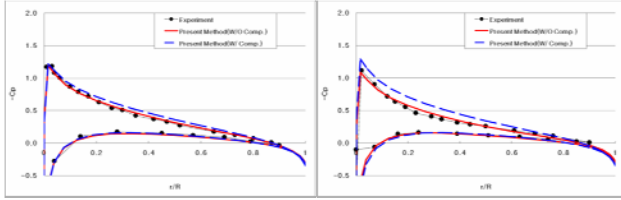
Fig. 4. Pressure distributions in hover (N= 1,250 RPM, Collective Pitch = 5 deg)

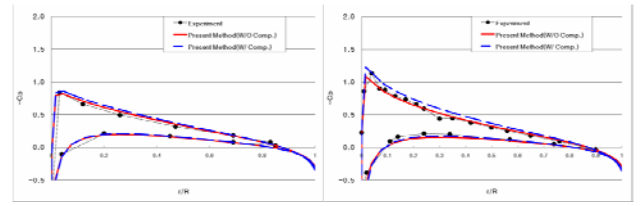(a) r/R=0.5 (b) r/R=0.8

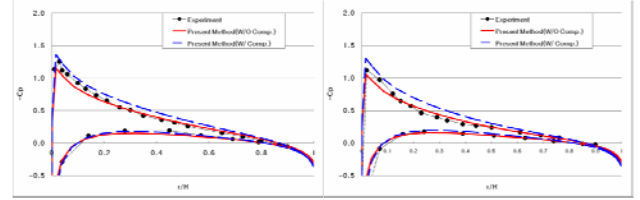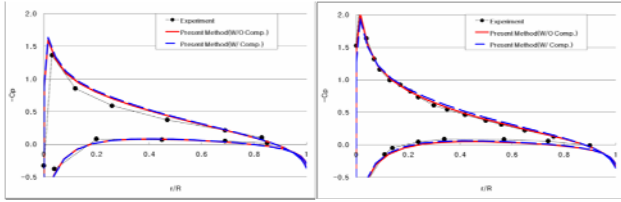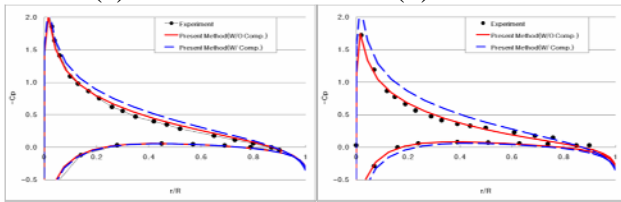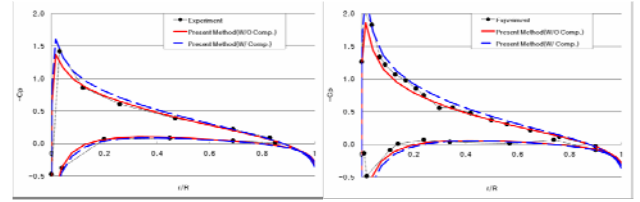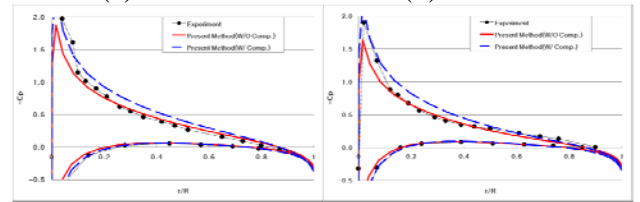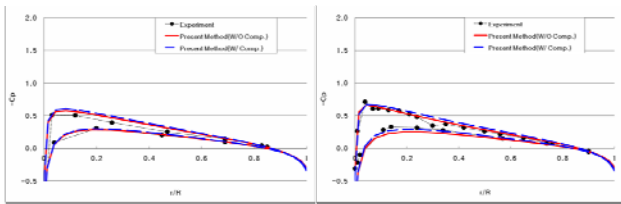(c) r/R=0.89 (d) r/R=0.96
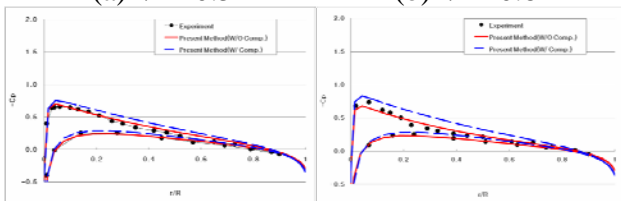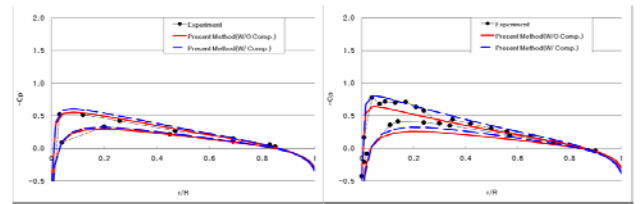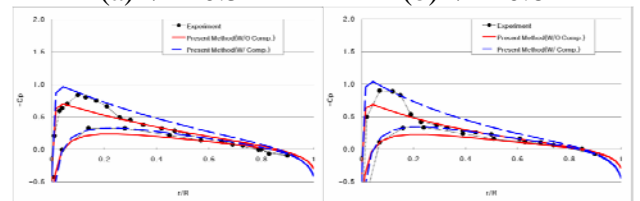
Fig. 5. Pressure distributions in hover
(N= 1,250 RPM, Collective Pitch = 8 deg)

(a) r/R=0.5 (b) r/R=0.8

(c) r/R=0.89 (d) r/R=0.96

Fig. 6. Pressure distributions in hover
(N= 1,250 RPM, Collective Pitch = 12 deg)

(a) r/R=0.5 (b) r/R=0.8

(c) r/R=0.89 (d) r/R=0.96

Fig. 7. Pressure distributions in hover
(N= 1,750 RPM, Collective Pitch = 5 deg)

(a) r/R=0.5 (b) r/R=0.8

(c) r/R=0.89 (d) r/R=0.96

Fig. 8. Pressure distributions in hover
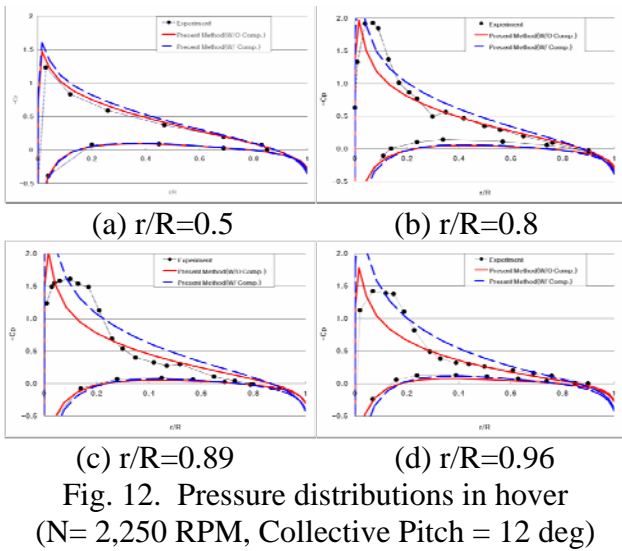(N= 1,750 RPM, Collective Pitch = 8 deg)

(a) r/R=0.5 (b) r/R=0.8

(c) r/R=0.89 (d) r/R=0.96

Fig. 9. Pressure distributions in hover
(N= 1,750 RPM, Collective Pitch = 12 deg)

(a) r/R=0.5 (b) r/R=0.8

(c) r/R=0.89 (d) r/R=0.96

Fig. 10. Pressure distributions in hover
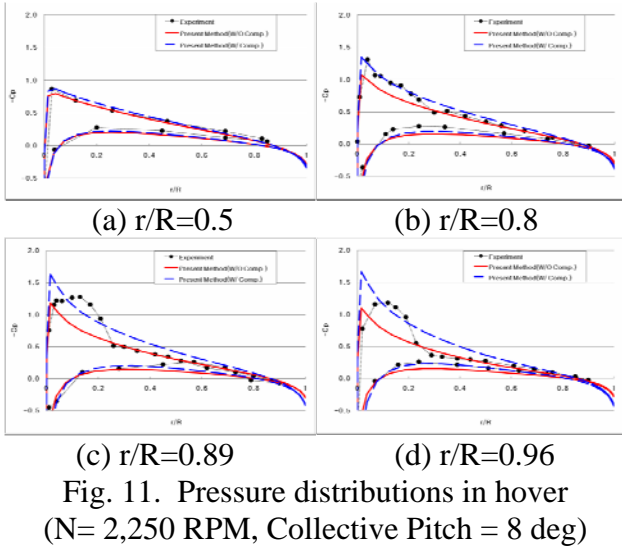(N= 2,250 RPM, Collective Pitch = 5 deg)

(a) r/R=0.5   (b) r/R=0.8

(c) r/R=0.89   (d) r/R=0.96

Fig. 11. Pressure distributions in hover
(N= 2,250 RPM, Collective Pitch = 8 deg)

(a) r/R=0.5   (b) r/R=0.8

(c) r/R=0.89   (d) r/R=0.96

Fig. 12. Pressure distributions in hover
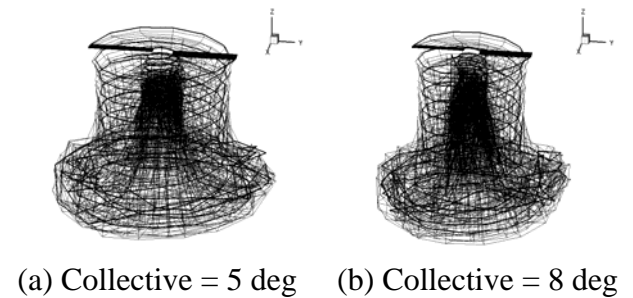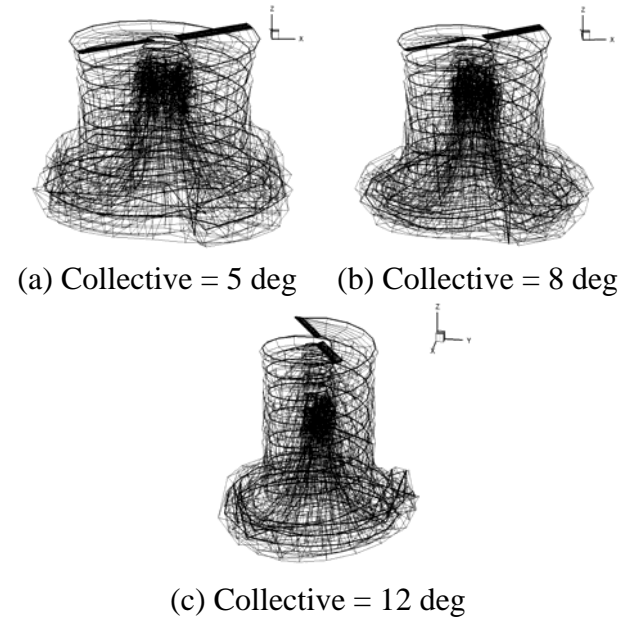(N= 2,250 RPM, Collective Pitch = 12 deg)

Table 1 Result of Hovering

Case	N (rpm)	Collective Pitch(deg.)	C_T Experiment	Present method	Deviation (%)
1		5	0.00213	0.002283	7.18
2				0.002374	11.46
3	1,250	8	0.00459	0.004653	1.37
4				0.004847	5.60
5		12	0.00796	0.006871	13.68
6				0.007026	11.73
7		5	0.00218	0.002316	6.24
8				0.002658	21.93
9	1,750	8	0.00455	0.004352	4.35
10				0.004844	6.46
11		12	0.00807	0.007125	11.71
12				0.008137	0.83
13		5	0.02	0.002206	88.97
14				0.002893	85.54
15	2,250	8	0.00462	0.004137	10.45
16				0.005389	16.65
17		12	0.00792	0.007159	9.61
18				0.009254	16.84

(a) Collective = 5 deg   (b) Collective = 8 deg

(c) Collective = 12 deg
Fig. 13. Wake shape in hover (N= 1,250 RPM)

(a) Collective = 5 deg   (b) Collective = 8 deg

(c) Collective = 12 deg
Fig. 14. Wake shape in hover (N= 1,750 RPM)

(a) Collective = 5 deg   (b) Collective = 8 deg
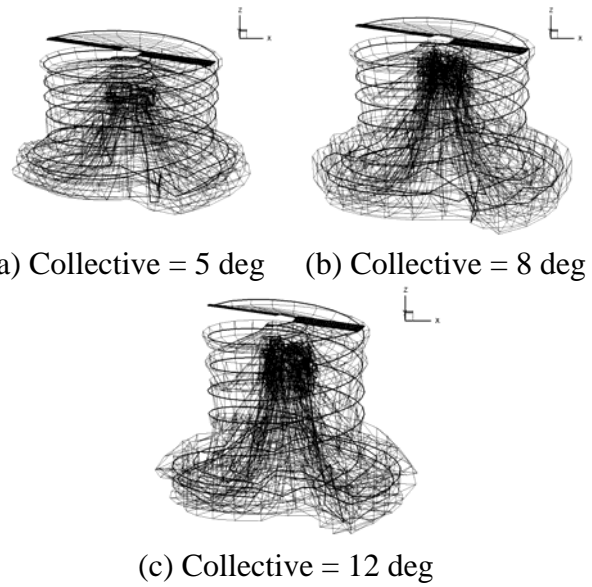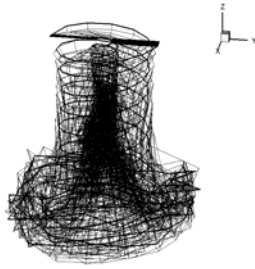
(c) Collective = 12 deg

Fig. 15. Wake shape in hover (N= 1,750 RPM)

3.2 Forward Flight

Figure 16 shows the geometry of UH-60 rotor[8] for the calculation of aerodynamic analysis in forward flight. There are 4 blades. Radius of the UH-60 rotor is 26.83ft. Solidity ratio of the rotor is 0.0826. Blade tip sweep(aft) is 20 degree. Blade chord length is 20.76/20.965 in.. Nominal rotor speed is 258 rpm. And the Section airfoils are composed of SC1095 and SC1094R8. Fig. 17 shows the geometry of UH-60 rotor blade. Fig. 18 shows the lift coefficient at 0.865R as the weight coefficient is 0.13. The result of the present method is matched well. Fig. 19 shows the wake shape of the UH-60 rotor.
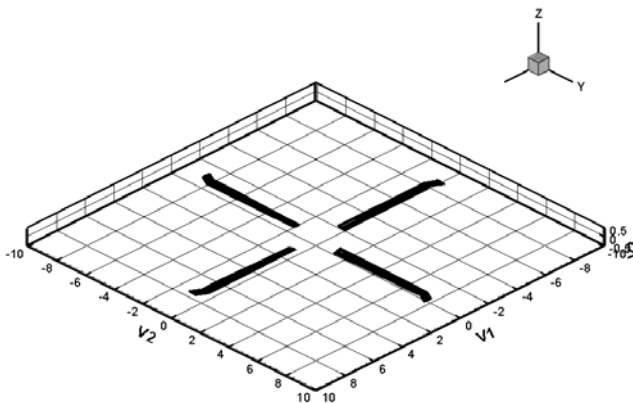

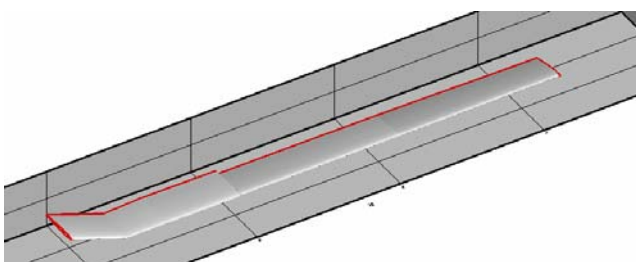Fig. 16. Geometry of UH-60 rotor

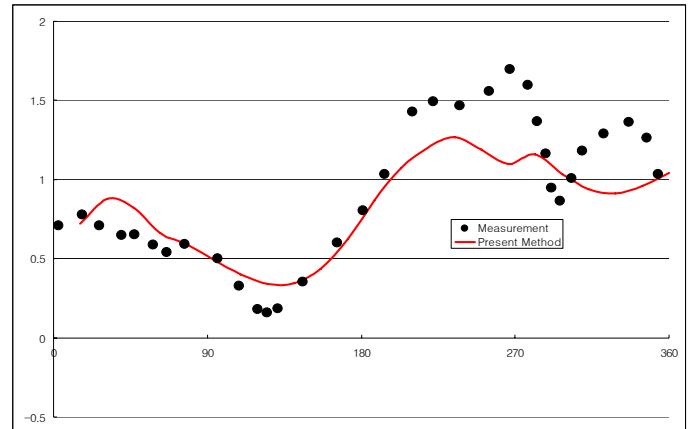Fig. 17. Blade geometry of UH-60 rotor

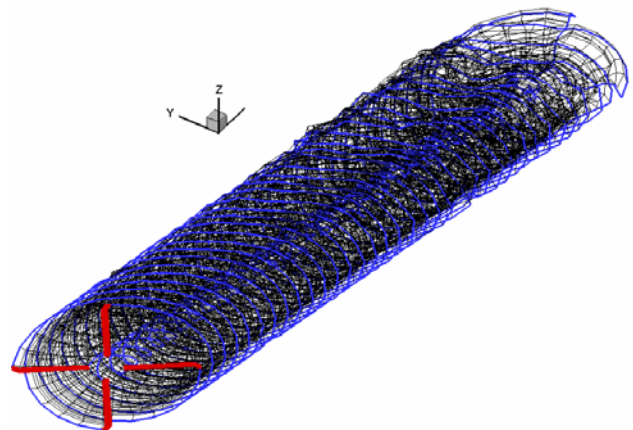Fig. 18 Blade section lift coefficient at 0.865R with weight coefficient 0.13

Fig. 19. Wake shape in forward flight of UH-60 rotor

4 Conclusions

Time-domain panel method and free wake were used to aerodynamic analysis and wake simulation of the helicopter rotor in hover and in forward flight. Time-domain panel method was assumed incompressible, irrotational flow, and using the source-doublet. The present method utilizes the time-stepping loop to analyze the aerodynamic characteristics and wake simulation of the helicopter rotor. The wake is calculated as part of the solution with no special treatment. The slow starting method was adopted in order to apply the inflow model

for the reasonable shape of wake. The results of present method were compared with experimental results in hover and in forward flight. Results of aerodynamic analysis with present method were satisfied compared to the results of experiment in hover and in forward flight. Time-domain panel method is considerably efficient, and present method can be used to inverse design and aerodynamic analysis of the helicopter rotor.

References

[1] Leishman, J. G, *Principles of HELICOPTER AERODYNAMICS*, 2nd edition, Cambridge Aerospace Series, 2006.

[2] Johnson, W., *Helicopter Theory*, Dover Publications, INC., 1994.

[3] Katz, J. and Plotkin, A., *Low-Speed Aerodynamics*, 2nd Ed., Cambridge University Press, New York, 2001.

[4] Done, G. and Balmford, D., *Bramwell's Helicopter dynamics*, Butterworth Heinemann, Oxford, 2001.

[5] Liu, P., "A Time-Domain Panel Method for Oscillating Propulsor with Both Chordwise and Spanwise Flexibility," Ph. D. Thesis, Faculty of Engineering & Applied Science, Memorial University of Newfourd St. John's, 1996.

[6] Maskew, B., *VSAERO User's Manual* (Revision E.5), Analytical Methods, Inc., Apr. 1994.

[7] Caradonna, F. X., and Tung, C., "Experimental and Analytical Studies of a Model Helicopter Rotor in Hover," NASA TM-81232, 1981.

[8] C. P. Coleman, and W. G. Bousman, "Aerodynamic Limitations of the UH-60A Rotor," NASA TM 110396, 1996

Copyright Statement